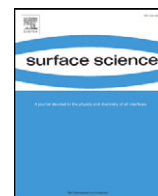




Contents lists available at ScienceDirect

Surface Science

journal homepage: www.elsevier.com/locate/susc

Novel PdAgCu ternary alloy as promising materials for hydrogen separation membranes: Synthesis and characterization

Ana M. Tarditi, Laura M. Cornaglia*

Instituto de Investigaciones en Catálisis y Petroquímica (FIQ, UNL-CONICET), Santiago del Estero 2829, 3000 Santa Fe, Argentina

ARTICLE INFO

Article history:

Received 3 June 2010

Accepted 1 October 2010

Available online xxx

Keywords:

Palladium based ternary alloys

Surface segregation

Hydrogen separation membrane

ABSTRACT

The use of the sequential electroless plating method allowed us to obtain the PdAgCu ternary alloy on top of dense stainless steel (SS) 316 L disks. The XRD analysis indicated that initially the nucleation of the two phases of the alloy (FCC and BCC) takes place, but the FCC/BCC ratio increases with the annealing time at 500 °C in H₂ stream. After 162 h, the film contained only the FCC phase, which presents promising properties to be applied in the synthesis of hydrogen selective membranes. SEM cross-section results showed that a dense, continuous, defect-free film was deposited on top of the SS support, and the EDS data indicated that no significant gradient was present on the thickness of the film. XPS and LEIS allowed us to determine that Cu and Ag surface segregation takes place after annealing up to 500 °C/5 days. In the top-most surface layer, Ag enrichment takes place as determined by ARXPS experiments which can be the result of the lower surface tension of Ag compared to that of Cu and Pd. Increasing the annealing temperature results in an increase of the Ag surface segregation while the Cu concentration in the top-most surface layer decreases.

© 2010 Elsevier B.V. All rights reserved.

1. Introduction

In the last few years, ultra-pure hydrogen production has attracted the attention of many research groups. Various alternatives have been proposed, among which the introduction of a membrane to a catalytic reactor seems promising. The combination of separation and reaction processes in a single unit is expected to provide greater flexibility of operation as well as further enhancement in the system performance. The use of dense palladium-based membranes appears as a potential route to hydrogen separation from the mixture stream due to their high perm-selectivity to hydrogen. However, their actual implementation is limited by their low mechanical stability and their high costs. Composite membranes, formed by a thin palladium layer on top of a porous substrate (ceramic, glass, or stainless steel) constitute an economical option to overcome these limitations.

Pure palladium undergoes a phase transition when exposed to hydrogen at temperatures below 300 °C [1]. This phenomenon is undesirable because it causes irreversible embrittlement in the Pd film. Additionally, Pd films can be irreversibly poisoned by sulfur compounds and other feedstock poisons which produce inhibition of the H₂ transport in the membrane film [2]. The presence of other metals as silver, ruthenium, copper and gold, at specific concentrations, also enhances the hydrogen permeation flux with no negative effects on its selectivity [3]. PdCu alloys have generated much research, not only because they do not exhibit hydrogen embrittlement even at room

temperature, but also because PdCu alloys are more resistant to H₂S poisoning than pure palladium when the alloy is in the face-centered-cubic (FCC) phase. Morreale et al. [4] showed that FCC PdCu alloy foils presented declines in permeance of about 10% when exposed to 1000 ppm H₂S/H₂ at high temperature, while the body-centered-cubic (BCC) phase showed declines in hydrogen permeance of up to 99%. Mundschau et al. [5] found that FCC PdCu alloys only had a 20% decline in permeance when exposed to 20 ppm H₂S. The disadvantage of the FCC PdCu alloy membranes compared with the BCC is their low permeance, in comparison to palladium and other palladium alloys [6]. For this reason, the use of a PdCu alloy with the introduction of low concentrations of a third metal (Au, Ag, Ru, and Rh) could be successful in increasing the H₂ permeance and maintaining the H₂S tolerance of the alloy membrane [7]. At present, only a limited number of articles have been published on the synthesis and hydrogen permeation measurements of palladium base ternary alloy membranes. Uemiyama and co-workers [8] reported the synthesis of a dense PdAgRu/Al₂O₃ ternary alloy membrane by simultaneous electroless plating deposition. The ternary alloy presents a higher H₂ permeation when it is compared with a PdAg and a Pd membrane on top of the same substrate and similar thickness. The permeability of the ternary membrane is about three to four times higher than the Pd membrane. Ryi et al. [9] synthesized a long term PdCuNi ternary alloy membrane by sputtering followed by Cu-reflow method. The membrane was durable after several thermal cycles between room temperature and 500 °C in H₂. The authors propose that the durability of the membrane is mainly due to the stabilization of the α -phase of Pd–H even at room temperature.

* Corresponding author. Tel.: +54 342 4536861.

E-mail address: lmcornag@fiq.unl.edu.ar (L.M. Cornaglia).

Detailed information about the surface composition and structure of alloys plays an important role in the interpretation of their physical and chemical properties. The investigation of the phenomena of surface segregation is required to understand the behavior of alloys in a wide range of applications as catalysis and corrosion. It is well-known that the component distribution on the membrane surface and in the bulk influences its hydrogen permeation properties. Hence, a deeper understanding of the relationship between the surface states, including structure and composition of the membrane, and its hydrogen permeability may lead to the discovery of new materials which provide higher hydrogen permeation. The surface segregation in the PdCu alloy system has been studied on both single and polycrystalline crystals. Surface studies have shown that the top atomic layer of PdCu alloys is rich in Cu, whereas the near surface region (~7 atomic layers) is rich in Pd, as reported by Miller et al. [10]. These data were consistent with those reported by Loboda-Cackovic et al. [11] using Auger Electron Spectroscopy (AES) and Temperature-Programmed Desorption (TPD) of CO.

The bulk electronic properties of the PdAg system are well established in the literature. Several theoretical and experimental studies using XPS and UPS are available, regarding surface segregation effects. The surface enrichment of silver was reported in the case of PdAg alloys in a vacuum or inert atmosphere consistent with lower surface energy of silver. Interestingly, a reverse surface segregation of palladium in PdAg membrane after exposure to H₂ has been reported by Shu et al. [12]. Citing XPS results they claim that hydrogen chemisorption on palladium sites drives strong palladium segregation on the PdAg membrane surface. Bredesen and co-workers [13] used XPS and AES to study the surface segregation effects on PdAg composite membranes after operation. The Ag/Pd ratio increases for about 32% after testing at high temperature as was evidenced by both XPS and AES data. Recently, Bosko et al. [14] reported the effect of different annealing temperature in metal segregation in a PdAg/SS membrane. The XPS data gave an indication of Ag segregation to the Pd–Ag film surfaces.

The aim of this work was to fabricate and characterize a PdAgCu ternary alloy with the electroless deposition method. The samples were synthesized by the sequential electroless plating technique on top of non-porous stainless steel 316 L disks. The effect of the annealing time at 500 °C in H₂ on the alloy formation was investigated by XRD. The morphology of the as synthesized samples was also studied by SEM and EDS. ARXPS together with LEIS experiments were used to investigate the surface segregation in the near-surface region and in the top-most atomic layer. This is the first paper of a series of two. In the second one, the hydrogen permeation and selectivity of PdAgCu/SS disk membranes will be presented as a function of temperature and pressure.

2. Experimental

2.1. Sample synthesis

2.1.1. PdAgCu ternary alloy preparation

Non-porous stainless steel disks (NPSDD) (0.9 mm in diameter and thickness of 2 mm) were used to study the PdAgCu alloy synthesis conditions. Prior to any plating experiment, supports were cleaned in a basic solution consisting of 0.12 M Na₃PO₄, 12H₂O, 0.6 M Na₂CO₃ and 1.12 M NaOH using the procedure reported by Ma et al. [15]. After that, the disks were treated with an acidic solution HCl:HNO₃ with a molar ratio of 1.6 in order to generate some roughness on the surface of the substrates and facilitate the adhesion of the film, followed by oxidation at 500 °C for 12 h. Solutions for activation were prepared using tin (II) chloride dehydrate and palladium (II) chloride. The chemical composition of the plating solutions are shown in Table 1. The activation procedure consisted of first dipping the substrate in the tin chloride solution and then in palladium chloride solution with intermediate rinsing in water between the immersions. After dipping

Table 1

Chemical composition of Pd, Ag and Cu electroless plating solutions and plating conditions.

	Pd	Ag	Cu
PdCl ₂ (g/l)	3.6	–	–
AgNO ₃ (g/l)	–	0.5	–
CuSO ₄ ·5H ₂ O (g/l)	–	–	20
NH ₄ OH (ml/l)	650	650	–
Na ₂ EDTA·2H ₂ O (g/l)	67	67	30
N ₂ H ₄ 1 M (ml/l)	10	10	–
HCHO (37%) (ml/l)	–	–	14
NaOH (g/l)	–	–	20
EDA (ppm)	–	–	100
K ₄ Fe(CN) ₆ ·3H ₂ O (ppm)	–	–	35
(C ₂ H ₅) ₂ NCS ₂ Na·3H ₂ O (ppm)	–	–	5
pH	11	11	12
Temperature (°C)	50	50	25

the support in the chloride solution it was rinsing with a 0.01 M HCl solution to avoid re-oxidation of palladium. This cycle was repeated 3 times. Electroless plating technique (ELP) was used to coat the support with a continuous metallic film. Palladium, silver and copper were deposited by sequential electroless deposition using the bath compositions shown in Table 1. First, palladium was deposited in two steps during 60 min each, followed by a short Ag deposition of 8 min. After the Pd and Ag depositions, the samples were rinsed with water and dried at 120 °C overnight. The Cu plating was performed during 50 min on top of the Pd–Ag layers. Plating times for Pd, Ag and Cu were adjusted to achieve the desired metal composition. After electroless deposition of Cu, the samples were immediately immersed in 0.01 M HCl to neutralize any residual plating solution, followed by rinsing with DI water and ethanol to facilitate drying and prevent oxidation of the copper layer. The deposition of Pd or Ag on top of a Cu surface was found to be difficult because Cu on the surface partially or completely dissolves in the plating bath. Therefore, the first metal layer applied to the support was always Pd, then Ag and finally a Cu layer was applied on top of the Pd–Ag layers. The sample was then heated up to 500 °C in H₂ atmosphere in order to form a homogeneous palladium–silver–copper alloy by thermal diffusion. To obtain a higher film thickness, after the first annealing, a second set of Pd, Ag and Cu thin layers was applied followed by a second heat treatment.

2.2. Sample characterization

2.2.1. X-ray diffraction

The phase structure of the samples as a function of annealing time was determined by X-ray Diffraction. The XRD patterns of the films were obtained with an XD-D1 Shimadzu instrument, using Cu Kα (λ = 1.542 Å) radiation at 30 kV and 40 mA. The scan rate was 1–2° min⁻¹ in the range 2θ = 15–90°.

2.2.2. Scanning electron microscopy and energy-dispersive X-ray analysis

The outer surface and cross-section images of the samples were obtained using a JEOL scanning electron microscope, model JSM-35C, equipped with an energy dispersive analytical system (EDAX). For the cross-section views, the disks were placed in a plastic tube; then epoxy resin was added. After hardening, they were cut by the middle of the disks. The grinding was carried out with waterproof abrasive paper of 180, 280, 500, 800 and 1200 grit. The polishing was done with a ~1 μm-grade paste, and finally with a suspension of γ-alumina (50 nm). The grinding and the polishing cycles lasted 5 min; after each cycle, it was necessary to clean the samples with ethyl alcohol in ultrasonic bath.

2.2.3. X-ray photoelectron spectroscopy

XPS analyses were performed in a multi-technique system (SPECS) equipped with an Al-monochromatic X-ray source, and a hemispherical

PHOIBOS 150 analyzer operating in the fixed analyzer transmission (FAT) mode. The spectra were obtained using a monochromatic Al K α radiation ($h\nu = 1486.6$ eV) operated at 300 W and 14 kV. The pass energy for the element scan was 30 eV. The working pressure in the analyzing chamber was less than 5×10^{-10} kPa. The XPS analyses were performed on the annealing samples and after different treatments in the main chamber. Before introducing the samples in the main chamber of the spectrometer, they were heated up in ultrapure H₂ at 350 °C and 50 kPa in the load-lock chamber. The spectra of Pd 3d, Pd 3p, O1s, C 1s, Ag 3d, Ag 3p, Cu 2p, Fe 2p, and their corresponding Auger peaks plus the valence band regions were recorded for each sample. The data treatment was performed with the Casa XPS program (Casa Software Ltd, UK). The peak areas were determined by integration employing a Shirley-type background. Peaks were considered to be a mixture of Gaussian and Lorentzian functions. For the quantification of the elements, we used the sensitivity factors provided by the manufacturer.

By varying the take-off angle between the direction of the escaping photoelectron and the surface plane of the sample, it was possible to obtain the surface segregation trend in the near-surface region. The measurements under different angles were carried out by tilting the sample with respect to the analyzer. For each ARXPS experiment, measurements were performed at six different angles up to 64° to the surface normal. In order to study the effect of different annealing treatments in the surface segregation, the XPS spectra of Pd, Ag and Cu were recorded at room temperature after annealing the sample at different temperatures *in-situ* in the main chamber. All spectra were taken in medium area mode, with a spot area about 3 mm.

2.2.4. LEIS spectroscopy

LEIS analysis was performed using a differentially pumped ion source IQE 12/38 SPECS, in the multi-technique system (SPECS). The LEIS spectra were taken by using helium ions with energy of 1 keV and a current density of about 400 nA/cm² to keep the change in surface composition by helium sputtering very low. Reference samples of pure Pd, Ag and Cu obtained by electroless deposition were used for calibration of the LEIS signals and to obtain the sensitivity factors. For the quantitative estimates of the top layer composition, we compared the LEIS peak areas (Gaussian fits) at $E/E_0 = 0.79$ for Cu and $E/E_0 = 0.85$ for [Pd + Ag].

The surface concentration of an element A in the alloy could be determined from the LEIS spectra by:

$$C_A = \frac{I_A}{I_A + f_{A/B} \cdot I_B + f_{A/C} \cdot I_C} \quad (1)$$

where I_A , I_B and I_C are the intensities of the ions scattered at atoms A, B and C with concentrations C_A , C_B and C_C ; with $C_A + C_B + C_C = 1$, $f_{A/B}$ and $f_{A/C}$ are the ratios of the peak intensities of the pure metals. From the calibration with reference samples we found that $f_{Cu/Pd}$ and $f_{Cu/Ag}$ were similar (0.22 and 0.23, respectively).

Using this result, Eq. (1) can be rewritten as follows:

$$C_{Cu} = \frac{I_{Cu}}{I_{Cu} + f_{Cu/Ag} \cdot (I_{Ag} + I_{Pd})} \quad (2)$$

We used Eq. (2) to perform a quantification of the top-most surface layer composition as a function of annealing temperature.

3. Results and discussion

3.1. PdAgCu ternary alloy formation

The main characteristics of the synthesized samples are summarized in Table 2. The thickness of the deposited metal was determined by gravimetric method, the weight gain of the sample divided by the

Table 2
Samples studied in this work.

Sample	Support	Cycle	Thickness (μm)	Grain size (nm) FCC phase	Thermal treatment
PdAgCu1	Non porous disk	1	7.5 ± 0.2^a	24	500 °C/48 h/H ₂
PdAgCu2	Non porous disk	2	13.0 ± 0.2	32	500 °C/120 h/H ₂
PdAgCu3	Non porous disk	1	6.5 ± 0.2	40	500 °C/162 h/H ₂
PdCu	Non porous disk	1	6.1 ± 0.2^a	–	500 °C/120 h/H ₂

^a Thickness of the Pd alloy on top of the support, as determined by SEM.

product of the plated surface area and the metal density considering a theoretical alloy composition. This method gave an average thickness value for the membrane in good agreement with the thickness determined from SEM images.

3.1.1. XRD study

PdAgCu non-porous disks were prepared to determine the time and conditions needed to obtain a pure FCC alloy. Fig. 1A exhibits the XRD patterns for the PdAgCu1 sample after the metallic deposition, and then of the annealing at 500 °C during 48 and 120 h, respectively. In order to optimize the alloy formation the sample was heated in different steps. The as-prepared sample yielded the expected Pd, Ag and Cu diffraction patterns. After the first deposition of Pd and Ag, the peaks from the modified SS support (43.1° and 50.2°) were not detected in the patterns (not shown), which gave an indication that the features at 42.9° and 50.1° observed after Cu deposition could be assigned to Cu and do not come from the stainless steel substrate. After annealing at 500 °C for 48 h, the peaks of Pd, Ag and Cu vanished and it was possible to observe the formation of two alloy phases, the FCC and BCC of the PdCu binary alloy. When the annealing time increased, the FCC/BCC ratio also increased, which is consistent with the data reported in the literature for the PdCu binary alloy [16]. Although Ag was deposited between Pd and Cu no peaks corresponding to the PdAg binary alloy (about 38.5°, 44.6°, 65.2°, depending on the composition) were observed in the patterns even after 162 h up to 500 °C. The change in composition in an alloy is reflected by the shift in the diffraction line positions in agreement with the change in the lattice parameter.

The fraction of each phase (X_{BCC} and X_{FCC}) could be estimated from the integrated intensities of their main peaks. For the quantitative estimation of X_{BCC} and X_{FCC} , the (111) peak of the FCC and that (110) of the BCC were analyzed. In order to apply this procedure so as to obtain the total concentration of palladium in our ternary alloy, we assumed that as the Ag concentration in the bulk is low it does not introduce any considerable modification in the lattice parameter and therefore does not modify the data obtained from these expressions.

The concentration of Pd in each phase (FCC or BCC) was calculated from the FCC and BCC lattice constants “ a ” according to the following equations previously derived by Goldbach and co-workers for the PdCu binary alloy [17,18].

$$a_{\text{FCC}} = 0.36462 \text{ nm} + (2.44 \times 10^{-4} \text{ nm}) * X_{\text{PdFCC}} \quad (3)$$

$$a_{\text{BCC}} = 0.2845 \text{ nm} + (2.88 \times 10^{-4} \text{ nm}) * X_{\text{PdBCC}} \quad (4)$$

From these equations, the palladium concentration in each phase was obtained. Using that, the Pd total concentration in the alloy ($[Pd]_{\text{T}}$) was 57% and 63% after 48 h and 120 h, respectively. The increase of $[Pd]_{\text{T}}$ with annealing time could be related to the inter-metallic diffusion during the alloy formation. The information recorded on the XRD patterns comes from about 3 μm in depth [19].

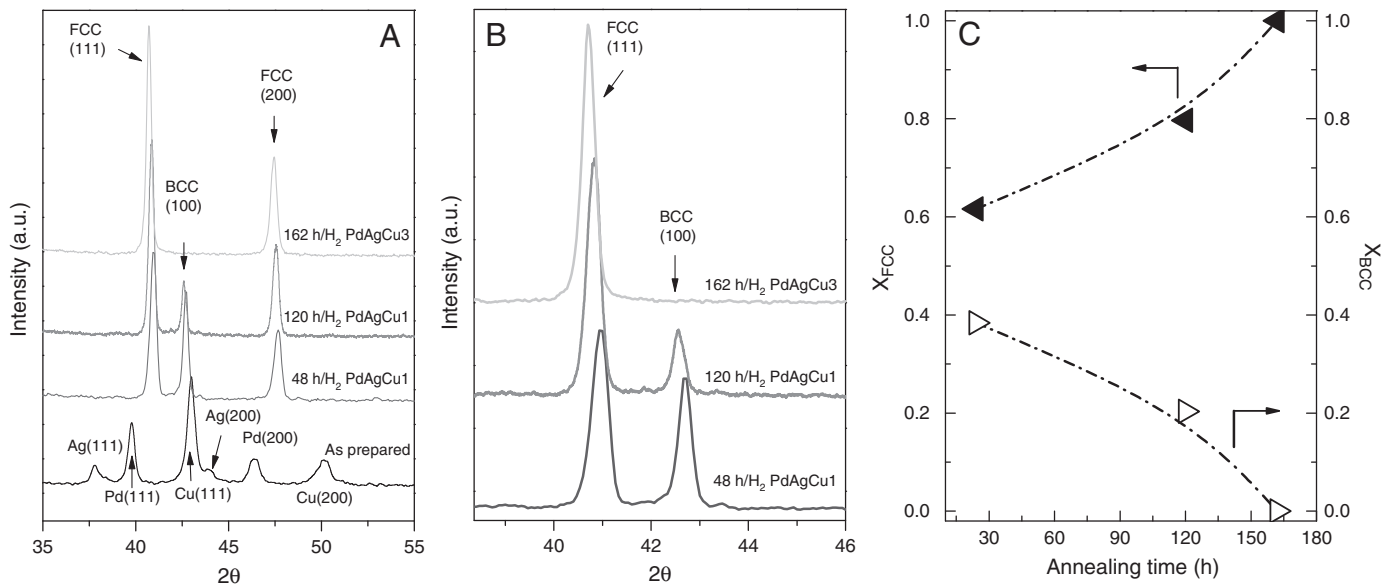


Fig. 1. X-ray diffraction patterns of the ternary alloy films. A) Patterns of the as synthesized samples and after annealing up to 500 °C in H₂ at different times. B) Short scan of the (111) FCC peak and the (100) BCC peak for the PdAgCu1 and PdAgCu3 samples. C) X_{FCC} and X_{BCC} as a function of annealing time.

These results suggest that Pd deposited in the first step migrates to the surface with annealing time. The $[\text{Pd}]_{\text{T}}$ after 120 h at 500 °C was close to that determined by weight gain, 69%. Note that the FCC (111) peak presents a slight shift with annealing time at lower 2θ , which is consistent with the increase in $[\text{Pd}]_{\text{T}}$. As shown in Fig. 1, after 162 h at 500 °C in H₂ only the feature corresponding to the FCC phase is observed in the XRD pattern of sample PdAgCu3, with a palladium

total composition of about 72% as determined from the lattice parameter. The lattice parameter for the FCC phase in the PdAgCu3 sample after annealing at 500 °C in H₂ for 162 h was 3.82 Å, which does not differ significantly from that reported for the FCC phase in the PdCu binary alloy (3.82–3.86 Å) [15].

Bredesen and coworkers reported that grain size growth may occur during deposition and/or membrane operation leading to an

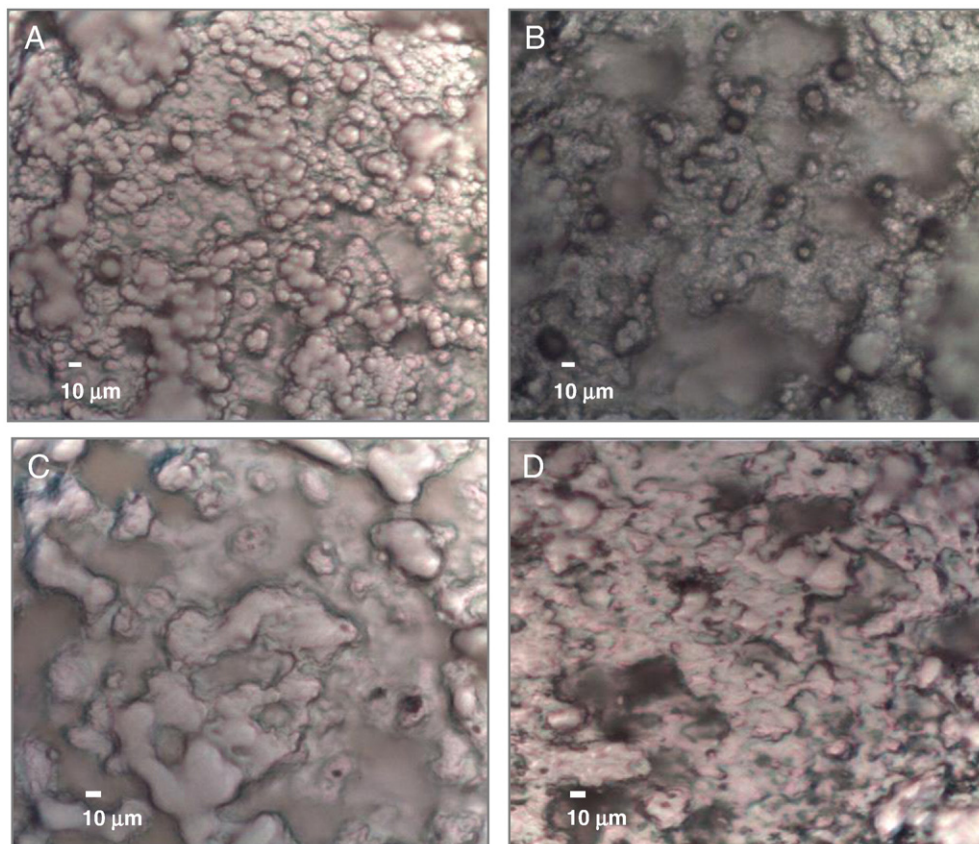


Fig. 2. Top views of the PdAgCu1 sample after Pd, Ag and Cu deposition (A, B, C, respectively). Pictures taken with an optical microscope. Surface of the PdAgCu1 sample after annealing up to 500 °C in H₂ (D).

increase in the hydrogen permeation flux for PdAg membranes [13]. The grain size may be estimated using Scherer's equation [20]:

$$D = \frac{k \cdot \lambda}{L \cdot \cos \theta} \quad (5)$$

where: L, k, λ and D are the microcrystalline size, Scherer's parameter (0.9), the wavelength (0.154 nm) and the FWHM of the reflection, respectively.

In the estimation of the grain size, the line broadening due to instrumental resolution is taken into consideration. Thus, the instrumental peak broadening (resolution function) was determined using Silicon standard material, and then subtracted from the measured peak broadening accordingly. As can be seen in Table 2, for PdAgCu1, the grain size of the FCC phase increases from 24 to 32 nm with an increase of annealing time from 48 h to 120 h. On the other hand, for the BCC phase, the grain size raises from 19 to 22 nm. Note that it is lower than the FCC grain size. In the same way, the grain size for the PdAgCu3 after 162 h at 500 °C increased by a factor of more than 1.6 with respect to PdAgCu1 after 48 h.

McCool and Li [21] observed grain size growth from 15 to 42 nm in a PdAg layer sputtered on alumina support upon heat treatment up to 500 °C on He stream. They found an increase in hydrogen permeance after grain growth in the composite membrane. The same effect was observed by Mekonnen et al. [22] who reported a grain size growth

with increasing temperature during the water gas shift testing. This result is in complete agreement with that reported by McColl and Li, indicating high temperature treatment as the main cause for grain growth in the membrane. Yuan et al. [18] reported an increase in the FWHM on both the FCC and BCC Bragg peaks of a PdCu alloy at low-temperature annealing, which could be due to smaller grain size.

3.1.2. Microstructure analysis of the PdAgCu alloy

The typical surface morphologies after the Pd, Ag and Cu plating are shown in Fig. 2A–C (these pictures were taken by an optical microscopy). As can be seen in Fig. 2C, the particles of Ag tend to form clusters, which grow in the direction normal to the support, as reported in the literature [19]. It should be noted that sample PdAgCu1 shows a smooth morphology after annealing at 500 °C in H₂ during 120 h (Fig. 3A). No dendritic growth was observed in the sample, which is consistent with the cross-section view observed by SEM where a smoothing surface could be seen (Fig. 3B). It is known from the literature that the Cu surface exhibits much smaller agglomerated particles than those observed in the Pd plating films where the typical cauliflower structure is present. After alloying, sample PdAgCu2 presents a uniform, smooth surface similar to that observed in PdCu alloys with similar Pd composition.

To verify the formation of a continuous layer on top of the NPSSD and study the chemical composition of the alloy, the cross section of the samples was analyzed by SEM and EDS. Fig. 3B shows the cross-

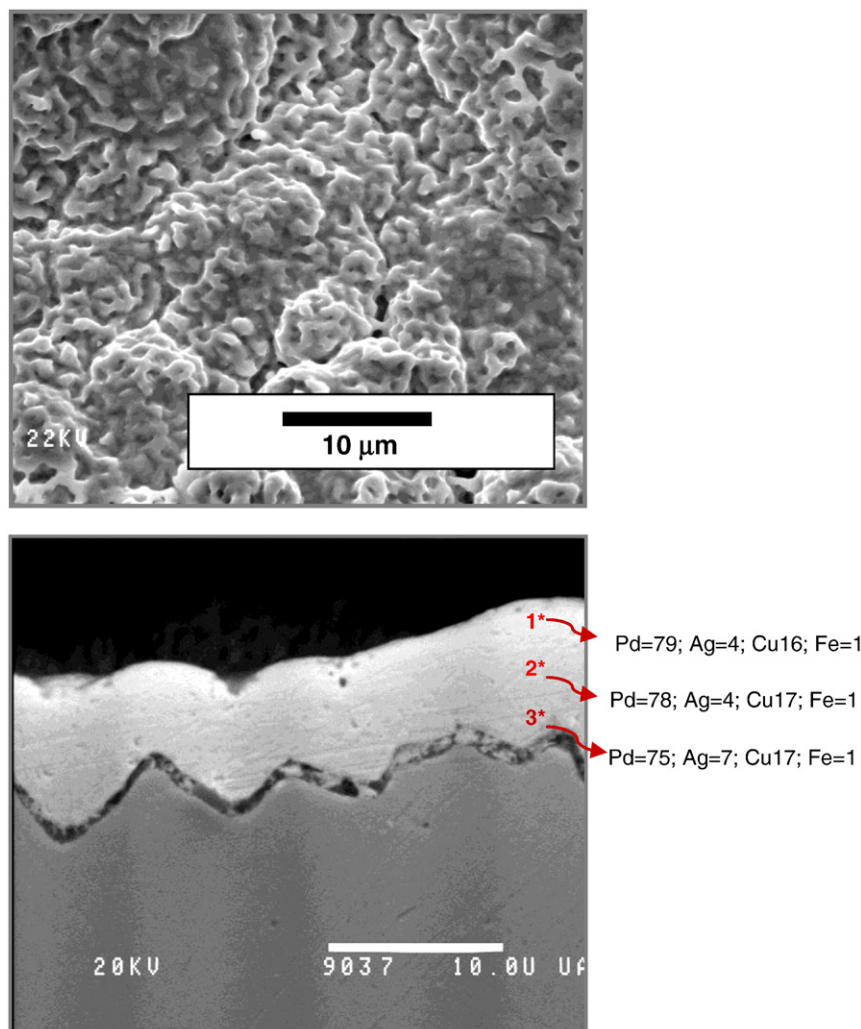


Fig. 3. SEM top view of the PdAgCu2 sample after annealing up to 500 °C in H₂ (A) and cross-section view of the PdAgCu1 sample after annealing up to 500 °C in H₂ during 120 h (B).

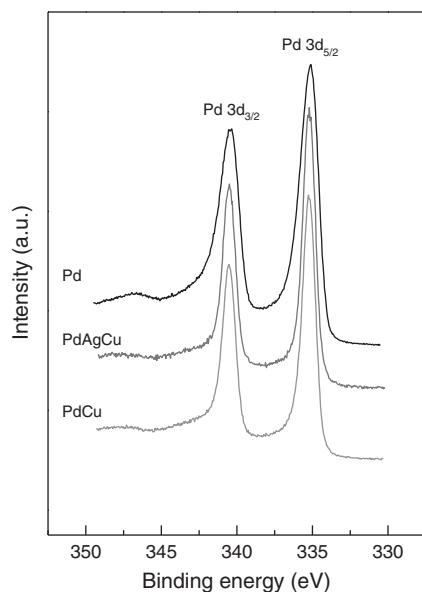


Fig. 4. Decrease in the FWHM of the Pd 3d_{5/2} peak upon alloying. A) Metallic Pd. B) PdCu alloy. C) PdAgCu alloy.

section image of the PdAgCu1 sample after annealing at 500 °C during 120 h in H₂. The alloy thickness on top of the NPSSD after one cycle of deposition was 7–8 μm (Fig. 3B). The cross-section view shows a homogeneous, continuous, defect-free deposition of the alloy. It is known from the literature that the silver deposition by electroless deposition results in a relatively heterogeneous surface coverage with large Ag dendritic clusters that tends to grow perpendicular to the surface [23]. However, no silver dendritic growth was observed in the ternary alloy studied in this work, as can be seen in Fig. 4. This might have resulted from the fact that, in our case, the silver composition is low (about 8%). Note that the sample presented a smooth surface morphology similar to that obtained in Pd and PdCu samples synthesized by electroless plating [24]. EDS spot scans were performed at various points in the layer to determine if a uniform alloy was produced by annealing. The chemical atomic composition determined from EDS scans of the sample PdAgCu1 was 75%Pd, 3%Ag and 21%Cu; no significant gradient was present in the film. This composition is consistent with that determined by XRD to the PdAgCu3 sample after annealing during 162 h. However, the existence of very small concentration gradients could not be excluded. Note that at the three points shown in Fig. 3B a low amount of Fe (~1%) was observed. Considering the fact that the Tamman temperature of the 316 L SS (550 °C) is higher than the annealing temperature used in the thermal treatment (500 °C), it is most likely that only a short-extension diffusion takes place. In the case of a Pd alloy/SS membrane, a diffusion barrier is usually introduced in order to avoid the diffusion of the SS components (Fe, Ni, and Cr).

3.1.3. Preliminary hydrogen permeation data

Our preliminary results using a PdAgCu/PSS disk membrane (0.2 μm grade support), prepared following the same procedure as the NPSSD samples, indicated that the PdAgCu ternary alloy exhibits a promising behavior for hydrogen separation. The membrane presents a hydrogen permeation flux of about $3.5 \times 10^{-2} \text{ mol s}^{-1} \text{ m}^{-2}$ at 450 °C and 100 kPa and H₂/N₂ ideal selectivity as high as 10,000 with an alloy film thickness of about 25 μm. A comparison with data reported in the literature, for both BCC and FCC PdCu membranes, is shown in Table 3.

3.2. Surface segregation study

It is known that the physical–chemical properties of the metallic alloy surfaces differ markedly from those of the bulk composition, and that this is mainly due to the surface segregation of one of the alloy components on the surface [25]. The surface segregation of one of the alloy metals plays an important role on the hydrogen adsorption and consequently, in the permeation properties of a palladium-based membrane [12]. In order to study the surface segregation in the annealing conditions used to prepare our samples, X-ray photoemission together with LEIS spectroscopy were employed to determine the composition of the near-surface region and top-most surface layer of the samples, respectively.

3.2.1. Near-surface region composition after alloy formation

In the XPS spectrum, in addition to the Pd, Ag and Cu characteristic features, only O and C peaks could be seen on the surface and no signal from the stainless steel (Fe, Ni, and Cr). The binding energy and the FWHM of the Pd 3d_{5/2}, Ag 3d_{5/2} and Cu 2p_{3/2} peaks are shown in Table 3. As can be seen in the table, the chemical composition of the PdAgCu1 sample after annealing up to 500 °C in H₂ during 120 h was 52.9% Pd, 23% Ag and 24.1% Cu, which shows a surface co-segregation of Ag and Cu with respect to the bulk composition determined by EDS (Table 3). Note that the extent of the Ag segregation is higher than the Cu segregation driven by its lower surface tension. The PdAgCu2 sample shows a similar Ag and Cu segregation as reported for the PdAgCu1 sample (Table 4).

The core-level binding energy shift is often used to study the electronic redistribution or charge transfer upon alloying [26–28]. The binding energy for the Pd 3d_{5/2} feature did not present a significant shift with respect to that of metallic Pd (BE = 335.1 ± 0.1 eV), while the Cu 2p_{3/2} peak showed a chemical shift to lower binding energies, 0.2 and 0.8 to the ternary and binary alloy, respectively. On other hand, the binding energy of the Ag 3d_{5/2} peak decreases in the PdAgCu ternary alloy compare to the metallic Ag. It was reported that the Cu chemical shift is caused by a strong interaction between palladium and copper in which bonds between the “sd” levels of Pd and resonant “dsp” levels of Cu are formed [29]. A redistribution of electrons between d and sp levels takes place. The originally empty conduction band levels of Cu become partially occupied upon alloying whereas Pd losses more or less a part of its “sd” metallic character through Cu. Behm and co-workers [30] reported a chemical shift of the Ag 3d_{5/2}

Table 3 Preliminary permeation data of PdAgCu/PSSD membranes compared with literature data.

Membrane	Thickness (μm)	Permeability [mol s m ⁻² Pa ^{-0.5}]	H ₂ /N ₂ Ideal selectivity	Temperature (°C)	Reference
PdCu _{BCC} /ZrO ₂ -α-Al ₂ O ₃	1.5	5.7×10^{-9}	93	450	[6]
PdCu _{FCC} /ZrO ₂ -α-Al ₂ O ₃	3.5	1.2×10^{-9}	>7000	350	[6]
PdCu _{FCC} /ceramic	5.5	2.5×10^{-9}	42	350	[18]
PdCu _{BCC} /ceramic	3.0	3.5×10^{-9}	—	500	[17]
PdAgCu _{FCC} /PSSD ^a	25	5.4×10^{-9}	>10,000	450	This work

^a Al₂O₃ modified porous stainless steel disk.

Table 4
Surface and bulk relative concentrations of the samples.

Sample	BE (eV)			FWHM (eV)			(% XPS)			(% EDS)		
	Pd 3d _{5/2}	Ag 3d _{5/2}	Cu 2p _{3/2}	Pd 3d _{5/2}	Ag 3d _{5/2}	Cu 2p _{3/2}	Pd	Ag	Cu	Pd	Ag	Cu
PdAgCu1	335.3	368.1	931.9	0.91	0.95	1.14	52.9	23	24.1	79	4	16
PdAgCu2	335.2	367.9	931.8	0.89	0.89	1.21	43.1	19.6	37.3	65	7	28
PdCu	335.1	–	932.3	0.94	–	1.08	62.3	–	37.7	76	–	24
Pd ^a	335.1	–	–	1.23	–	–	–	–	–	–	–	–
Ag ^a	–	368.6	–	–	0.96	–	–	–	–	–	–	–
Cu ^a	–	–	932.6	–	–	1.08	–	–	–	–	–	–

^a Reference samples prepared by electroless plating.

peak with the alloy formation in a PdAg film due to an electronic modification. For the PdAg system, Chae et al. [31] reported that there exists a shift to higher binding energies in the Pd 3d_{5/2} peak whereas in the Ag 3d_{5/2} peak the shift is to lower binding energies due to a charge transfer of electrons between the alloy components. Applying the charge distribution model, they estimated the direction and amount of the charge transfer in the alloy. The results of such estimation show that upon alloying there is a decrease in sp-like conduction electrons and an increase in the number of d-electrons at the Pd site.

As regards multi-component alloys, only a few articles in the literature have analyzed the core-level surface characterization related with the alloy formation. Lee and al. [32] reported a XPS study about the formation of the MoRuRhPd alloy. They found a shift to higher binding energies of the Pd 3d_{5/2} peak with respect to the Pd metallic binding energy, which is related to the final state redistribution when a chemical bonding between Pd and Mo takes place.

An additional point of interest is that the FWHM of the Pd 3d_{5/2} peak decreases with the alloy formation, from 1.23 ± 0.05 eV to 0.91 ± 0.05 eV for pure Pd and Pd in the ternary alloy, respectively (Fig. 4). The drop in the FWHM is followed by a decrease in the peak asymmetry, while the symmetry of the Ag 3d_{5/2} and Cu 2p_{3/2} remains unchanged. Hedman and co-workers [33] reported a decrease in the FWHM of Pd 3d_{5/2} with the increase in Cu concentration in the alloy, due to the modification of the local density of states in the Fermi level, which is consistent with the shift in the Cu 2p_{3/2} peak. The chemical core-level shifts together with the Pd 3d_{5/2} FWHM changes observed in both the PdAgCu1 and PdAgCu2 samples are a good indication of the surface alloy formation, in agreement with the XRD data.

Angle-resolved XPS provides important information regarding the composition gradient that could exist within the near-surface region. Fig. 5 summarizes the ARXPS data obtained from the PdAgCu2 sample after annealing up to 500 °C during 120 h. Note that the Cu concentration decreases with increasing emission angle (between the direction of the escaping photoelectron and the normal to the surface), while the Ag concentration increases in the same way. No significant Pd gradient was observed in these experiments (Fig. 5). This Ag enrichment at the surface observed in the ternary alloy is mainly due to the fact that Ag has a lower surface tension than Cu and Pd (1, 1.4 and 1.7 J/m², respectively [34]). In a Pd₇₀Cu₃₀ binary alloy, Miller et al. [9] found a Pd enrichment in the XPS-accessible near-surface region with respect to the bulk composition. Using LEIS, they also observed copper enrichment in the top-most surface layer. On the other hand, for a Cu₈₀Ag₂₀ alloy it has been reported that a Ag surface segregation takes place, even at room temperature [35,36]. Katamaya et al. [35] pointed out that the segregation at room temperature could be connected with the lower sublimation energy and with the large atomic size of silver. The enrichment of Ag at the surface has also been observed by Hoffman et al. [36] using Auger spectroscopy as a function of temperature. In the case of PdAg alloys, silver segregation is often detected [14,37]. Our ARXPS results are quite different from the trend reported by Miller et al. for a binary PdCu alloy [10], i.e., we see a Cu enrichment by XPS and a decrease in the Cu concentration to the nearest surface region. This could be due to the presence of Ag in the alloy. Gargano et al. [38] used the mean-field Bozzolo–Ferrante–Smith (BFS) model for the determination of the segregation profile of two ternary alloys (Cu–Al–Ni and Cu–Ag–Au). In the former alloy,

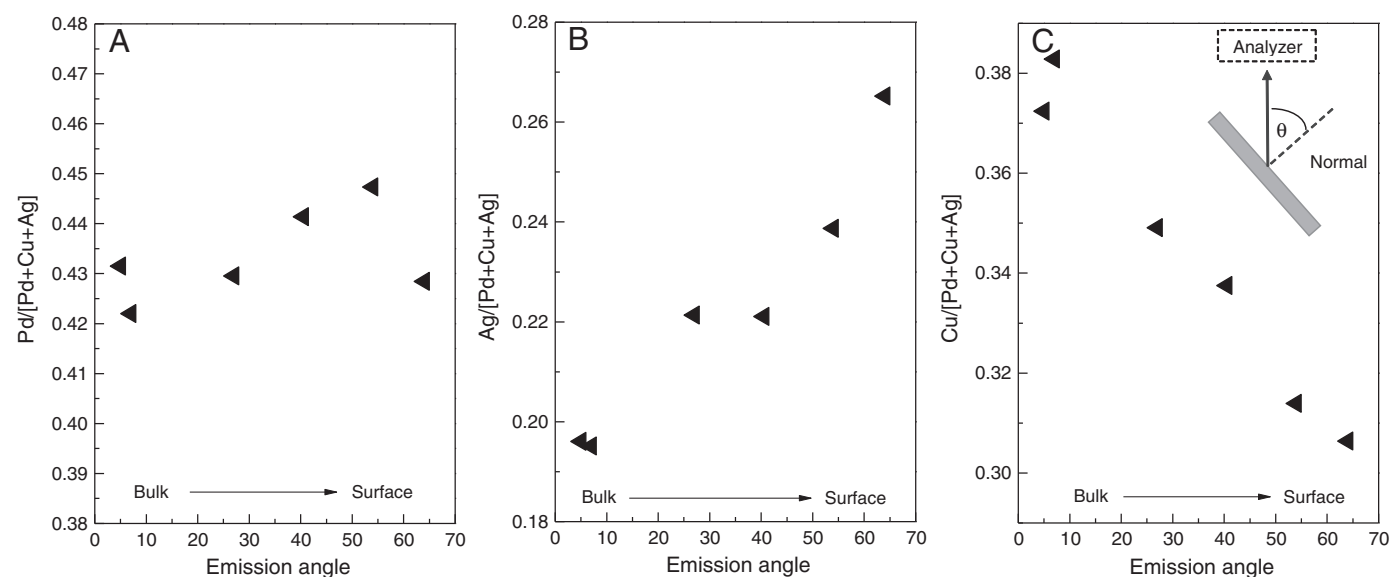


Fig. 5. ARXPS study of the PdAgCu2 sample. A) Pd, B) Ag and C) Cu profiles in the near-surface region after annealing up to 500 °C in H₂. Data taken at room temperature.

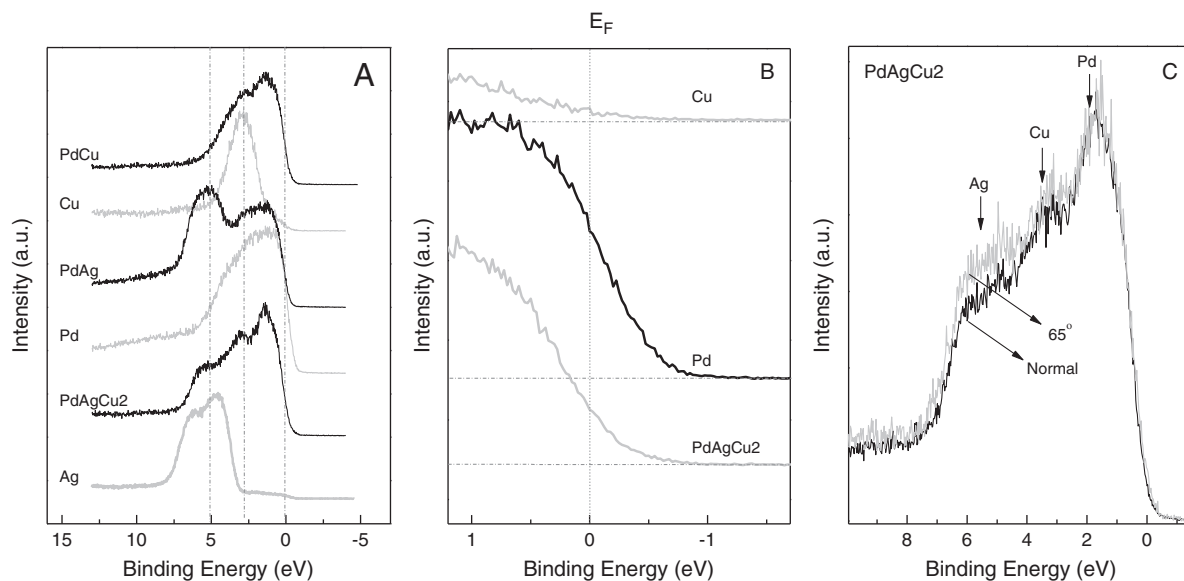


Fig. 6. Valence band spectrum of the Pd, Cu, Ag and the PdCu and PdAgCu alloys. Data taken at room temperature.

they found a different segregation profile with respect to the binary alloys due to interaction between minority components.

3.2.2. Valence band spectrum

The behavior of the valence-band spectra for the PdAgCu2 sample is shown in detail in Fig. 6. The spectrum of the sample clearly shows three well-resolved bands at about 5.5, 2.8 and 1.5 eV assigned to Ag, Cu and Pd, respectively (Fig. 6A). Close to the Fermi level, we can observe the Pd 4d bands, which extend over a region of about 5 eV below the Fermi level as reported in the literature [33]. The pure silver spectrum has two features at about 4.5 and 6.5 eV, corresponding to the Ag sp band and d state band, respectively [12]. Finally, copper has a narrow d band located between 2 and 5 eV from the Fermi level as reported by Hedman and coworkers [33]. Upon alloying, the Pd d-band moves away from the Fermi level and becomes narrower

(Fig. 6B). Hedman and co-workers used UPS to show that the higher the Pd content of a PdCu alloy, the more electron density exists just at and below the Fermi level (E_F). This decrease in the local density of states in the Fermi level is in line with the decrease in the asymmetry of the Pd $3d_{5/2}$ peak (Fig. 6).

An examination of the valence band spectra of sample PdAgCu2 as a function of the emission angle shows a slow increase in the Ag band while the Pd bands remains unchanged (Fig. 6C). These results are in agreement with ARXPS data of core level (Fig. 5).

3.2.3. Top-most surface layer composition after alloy formation

Low energy ion scattering spectroscopy (LEIS) was used to determine the composition of the sample top-most surface layer. Fig. 7 shows a characteristic spectrum taken at room temperature for the PdAgCu1 sample obtained after annealing up to 500 °C during

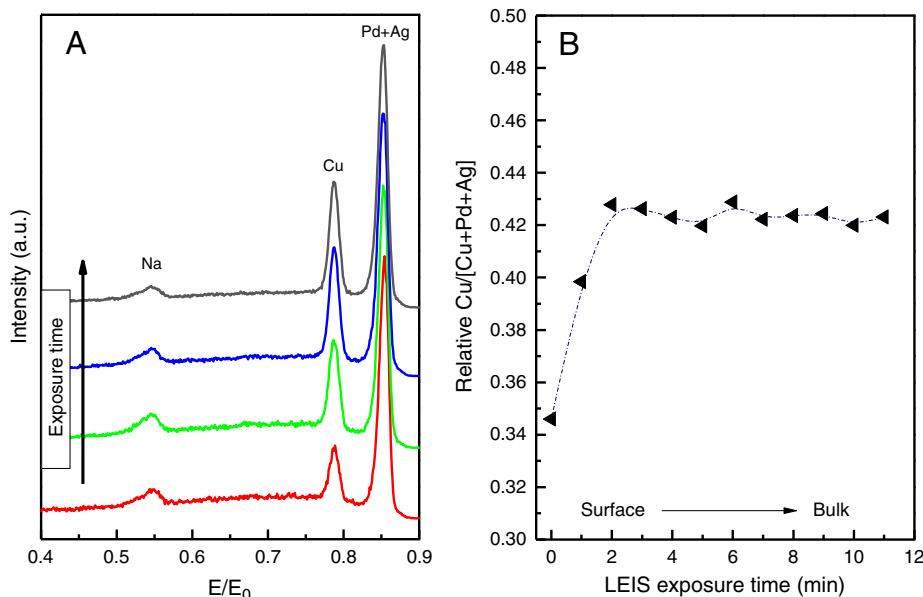


Fig. 7. A) Characteristic LEIS spectrum of the PdAgCu2 ternary alloy. B) Cu tends in the top most surface region. Data taken at room temperature.

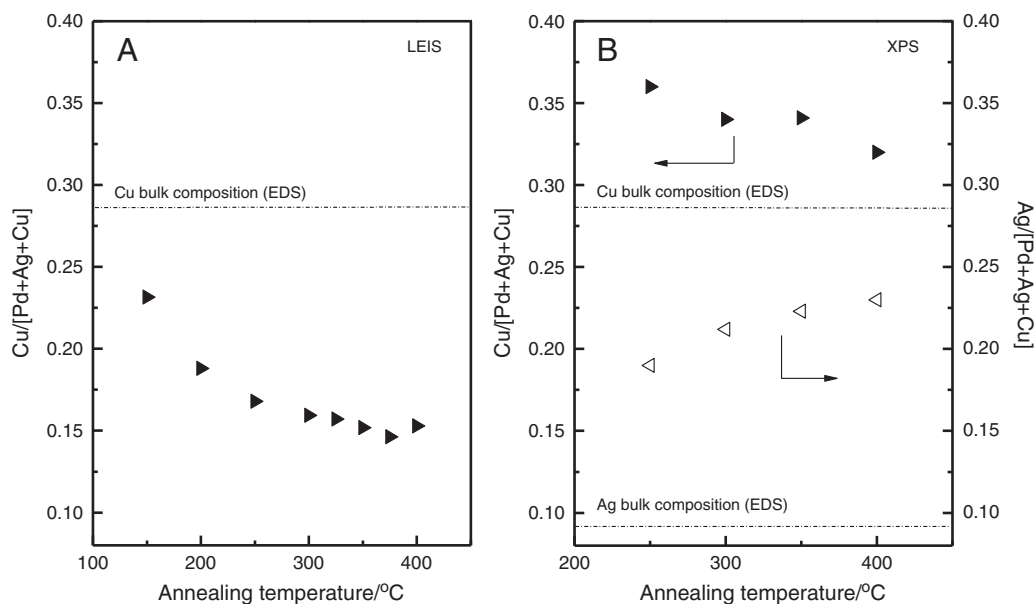


Fig. 8. A) Cu top-most surface layer composition determined by LEIS as a function of annealing temperature of the PdAgCu₂ sample. B) Ag and Cu near surface composition as a function of annealing temperature. (XPS data were taken at room temperature and LEIS data were taken at annealing temperature).

120 h in H₂ stream. The spectrum exhibits two main peaks at $E/E_0 = 0.79$ and 0.85 assigned to Cu and [Pd + Ag], respectively. Note that the Pd and Ag peaks could not be resolved under our experimental conditions due to the small difference between the masses. An additional feature tentatively assigned to Na ($E/E_0 = 0.55$) appears in the spectrum which could be originated from the compounds used in the sample preparation by electroless deposition. As mentioned previously, this technique could not resolve the Pd and Ag peaks; however, from the LEIS data it is possible to make a relative determination of the Cu composition on the top-most surface layer. Fig. 8B shows the relative Cu/[Cu + Pd + Ag] ratio as a function of LEIS exposure time which could give an indication of a relative depth profile in the near surface region due to sputtering effects. Note that the relative copper concentration increases with the successive scans, which suggests that a Pd and/or Ag enrichment in the top-most surface layer takes place (Fig. 7). These data are consistent with the ARXPS results where a Cu decrease on the external surface was observed while the Ag concentration increases (Fig. 5).

3.2.4. Effect of annealing temperature on surface segregation

The effect of the *in-situ* annealing temperature on the surface composition of the PdAgCu alloy was investigated using XPS and LEIS spectroscopy. The near surface region (XPS) and the top-most surface layer (LEIS) composition at annealing temperatures between 100 and 400 °C are summarized in Fig. 8. XPS data were taken at room temperature. First, the sample was annealed at the desired temperature and then cooled down to room temperature. On the other hand, the LEIS experiments were performed at high temperature. It was reported by Miller et al. [9] that the top layer compositions determined by LEIS clearly depend on the temperature at which the LEIS spectrum is obtained. As can be seen from the picture, the LEIS Cu/[Pd + Cu + Ag] ratio decreases with temperature in the same way as the XPS data. While the Cu surface composition of the near surface region (XPS) is always above the bulk composition determined by EDS, the Cu top-most surface layer composition (LEIS) is significantly lower than that of the bulk. This data are consistent with the data obtained by ARXPS where an Ag segregation on the top-most layer surface was evidenced (Fig. 5).

As can be seen from Fig. 8B, the Ag concentration in the near surface region slowly increases with the annealing temperature while the Cu concentration decreases. No significant modification in the

Pd near surface concentration was observed with temperature (not shown). According to Katamaya et al. [35], Ag enrichment was observed by LEIS in a Cu–20%Ag binary alloy even at room temperature. In complete agreement with these data, Abraham et al. [38,39] showed by Auger spectroscopy that a strong Ag segregation takes place at low temperature.

From the experimental data it can be concluded that as a result of annealing, Ag segregates to the top-most surface layer. Higher annealing temperature results in an increase of the Ag surface segregation while the Cu concentration in the top-most surface layer decreases. This could be a result of the lower surface tension of Ag with respect to the Cu and Pd.

4. Conclusions

Using the sequential electroless plating technique, it was possible to obtain a homogeneous, continuous, defect-free film of PdAgCu ternary alloy on top of dense stainless steel 316 L disks. Results of the annealing study for the formation of the alloy at 500 °C in H₂ showed that the nucleation of both phases (BCC and FCC) takes place. As the annealing time increases, the FCC fraction increases until the BCC phase disappears after 162 h at 500 °C, as evidenced by XRD.

The surface alloy formation was verified by the decrease in the Pd 4d density states in the valence band, which was consistent with the core-level chemical shift of the Cu 2p_{3/2} and Ag 3d_{5/2} features.

The near-surface region of the sample became enriched in Cu and Ag with respect to the bulk composition determined by EDS, showing that a co-segregation of both metals takes place in the annealing conditions used to prepare the ternary alloy. The top-most layer composition is silver-rich compared to the bulk composition as observed from ARXPS.

Increasing the annealing temperature results in an increase of the Ag surface segregation while the Cu concentration on the top-most surface layer decreases. This could be a result of the lower surface tension of Ag with respect to Cu and Pd.

Acknowledgements

The authors wish to acknowledge the financial support received from UNL, CONICET and ANPCyT. They are also grateful to ANPCyT for Grant

PME 8-2003 to finance the purchase of the UHV Multi Analysis System. Thanks are given to Elsa Grimaldi for the English language editing.

References

- [1] F.A. Lewis, *Platinum Met. Rev.* 40 (1996) 180.
- [2] J.K. Ali, E.J. Newson, D.W.T. Rippin, *J. Membr. Sci.* 89 (1994) 171.
- [3] Ø. Hatlevik, S.K. Gade, M.K. Keeling, P.M. Thoen, A.P. Davidson, J. Douglas Way, *Sep. Purif. Technol.* 73 (2010) 59.
- [4] B.D. Morreale, M.V. Ciocco, B.H. Howard, R.P. Killmeyer, A.V. Cugini, R.M. Enick, *J. Membr. Sci.* 241 (2004) 219.
- [5] M.V. Mundschaue, X. Xie, C.R. Evenson, A.F. Sammells, *Catal. Today* 118 (2006) 12.
- [6] F. Roa, J. Douglas Way, *Ind. Eng. Chem. Res.* 42 (23) (2003) 5827.
- [7] L. Semidey-Flecha, Ch. Ling, D. S. Sholl, Equation Detailed First-principles Models of Hydrogen Permeation Through PdCu-based Ternary Alloys. *J. Membr. Sci.* 362 (1–2) (2010) 384.
- [8] L. Wang, R. Yoshiie, S. Uemiya, *J. Membr. Sci.* 306 (2007) 1.
- [9] S.-K. Ryi, J.-S. Park, S.-H. Kim, D.-W. Kim, J.-W. Moon, *J. Membr. Sci.* 306 (2007) 261.
- [10] J.B. Miller, Ch. Matrangola, A.J. Gellman, *Surf. Sci.* 602 (2008) 375.
- [11] J. Loboda-Cackovic, M.S. Mousa, J.H. Block, *Vacuum* 46 (2) (1995) 89.
- [12] J. Shu, B.E.W. Bongondo, B.P.A. Grandjean, A. Adnot, S. Kaliaguine, *Surf. Sci.* 291 (1993) 129.
- [13] T.A. Peters, W.M. Tucho, A. Ramachandran, M. Stange, J.C. Walmsley, R. Holmestad, A. Borg, R. Bredesen, *J. Membr. Sci.* 326 (2009) 572.
- [14] L.M. Bosko, J.B. Miller, E.A. Lombardo, A. Gellman, L.M. Cornaglia, Surface characterization of Pd–Ag composite membranes after annealing at different temperatures. Submitted to *J. Membr. Sci.* 2010.
- [15] Y.H. Ma, B.C. Akis, M.E. Aytrurk, F. Guazzone, E.E. Enqwall, I.P. Mardilovich, *Ind. Eng. Chem. Res.* 43 (2004) 2936.
- [16] A. Goldbach, L. Yuan, H. Xu, Impact of the fcc/bcc phase transition on the homogeneity and behavior of PdCu membranes, *Sep. Purif. Technol.* 73 (1) (2010) 65.
- [17] J. Yuan, A. Goldbach, H. Xu, *J. Phys. Chem. B* 112 (2008) 12692.
- [18] J. Yuan, A. Goldbach, H. Xu, *J. Membr. Sci.* 322 (2008) 39.
- [19] M.E. Ayrturk, Y.H. Ma, *J. Membr. Sci.* 330 (1–2) (2009) 233.
- [20] B.D. Cullity, *Elements of X-Ray Diffraction*, Second Edition, 1978.
- [21] B.A. McCool, Y.S.K. Lin, *J. Mater. Sci.* 36 (2001) 3221.
- [22] W. Mekonnen, B. Arstad, H. Klette, J.C. Walmsley, R. Bredesen, H. Benvik, R. Holmestad, *J. Membr. Sci.* 310 (2008) 337.
- [23] R. Bhandari, Y.H. Ma, *J. Membr. Sci.* 334 (2009) 50.
- [24] N. Pomerantz, Y.H. Ma, *Ind. Eng. Chem. Res.* 48 (2009) 4030.
- [25] O.M. Løvvik, S.M. Opalka, *Surf. Sci.* 602 (2008) 2840.
- [26] C.W. Yi, K. Luo, T. Wei, D.W. Goodman, *J. Phys. Chem. B* 109 (2005) 18533.
- [27] Y.S. Lee, Y. Jeon, Y.D. Chung, K.Y. Lim, C.N. Whang, S.J. Oh, *J. Korean Phys. Soc.* 37 (2000) 451.
- [28] S. Hufner, G.K. Wertheim, J.H. Wernick, *Solid State Commun.* 17 (1975) 417.
- [29] H. Gao, J.Y.S. Lin, Y. Li, B. Zhang, *J. Membr. Sci.* 265 (2005) 142.
- [30] Y. Ma, J. Bannmann, T. Diemant, R.J. Behm, *Surf. Sci.* 603 (2009) 1046.
- [31] K.H. Chae, Y. Lee, S.M. Jung, Y. Jeon, I.M. Croft, C.N. Whang, *Nucl. Instrum. Meth. B* 106 (1995) 60.
- [32] J.-Y. Lee, Y.J. Park, H.Y. Pyo, J.G. Kim, K.Y. Jee, W.H. Kim, Y. Jeon, *J. Alloys. Comp.* 298 (2000) 291.
- [33] N. Martenson, R. Nyholm, H. Calén, J. Hedman, *Phys. Rev. B* 24 (4) (1981) 1725.
- [34] G.V. Samsonov, A.N. Krasnov, *Fiziko Khimicheskaya Mekhanika Materialov* 2 (1966) 485.
- [35] I. Katamaya, F. Shoji, K. Oura, T. Hanawa, *Appl. Surf. Sci.* 33/34 (1988) 129.
- [36] M.A. Hoffman, S.W. Bronner, P. Wynblatt, *J. Vac. Sci. Technol. A* 9 (1991) 27.
- [37] M. Yamamura, K. Kaneda, T. Imanaka, *Catal. Lett.* 3 (1989) 203.
- [38] P. Gargano, H. Mosca, G. Bozzolo, *Phys. B* 404 (2009) 2769.
- [39] F.F. Abraham, C.R. Brundle, *J. Vacuum Sci. Technol.* 18 (1981) 506.